

## **Impedance spectroscopy analysis and structural of $\text{Ni}_{0.7}\text{Zn}_{0.3}\text{Fe}_2\text{O}_4$ samples synthesis by co-precipitation method at different temperature**

Abdulsamee Fawzi Abdul Aziz Albayati

Department of physics, College of Science, University of Tikrit, Tikrit, Iraq.

[abdulsamee\\_fawzi@yahoo.com](mailto:abdulsamee_fawzi@yahoo.com)

### **ABSTRACT**

In this study,  $\text{Ni}_{0.7}\text{Zn}_{0.3}\text{Fe}_2\text{O}_4$  was prepared by chemical deposition at temperatures of 700°C, 800°C, 900°C, 1000°C, 1100°C and 1200°C respectively, The various applications on the spectral and structural analysis of  $\text{Ni}_{0.7}\text{Zn}_{0.3}\text{Fe}_2\text{O}_4$  compounds, as observed by X-ray diffraction technique, show that all samples with spherical structure and interstitial intervals have the same Miller coefficients (2.958, 2.517, 2.422, 2.093, 1.717, 1.613, 1.481 and 1.279) nm. Spectral impedance is a tool for understanding the various contributions to electrical properties of semiconductors. Through complex, intricate and complex permutations, the contributions of grains and boundary grains were understood in the electrical characteristics of the samples. The spectral analysis of the impedance as a frequency function (1 kHz-5 MHz) was done for  $\text{Ni}_{0.7}\text{Zn}_{0.3}\text{Fe}_2\text{O}_4$  samples. it showed the imaginary part of the reluctance as a function of the complex impedance that shows Debye type of relation time. Cole-Cole plots (relation between real and imaginary parts for impedance complex) showed a non-Debye type of relaxation time of insulation.

**Keywords:** Ni-Zn ferrites, X-ray diffraction, dielectric constant measurements, impedance spectroscopy.

## تحليل الممانعة الطيفية والتركيبيية لنماذج $Ni_{0.7}Zn_{0.3}Fe_2O_4$ المحضرة بطريقة

### الترسيب الكيميائي عند درجات حرارة مختلفة

عبد السميع فوزي عبد العزيز البياتي

قسم الفيزياء, كلية العلوم, جامعة تكريت, تكريت, العراق.

[abdulsamee\\_fawzi@yahoo.com](mailto:abdulsamee_fawzi@yahoo.com)

#### المخلص

في هذا البحث تم تحضير مركب  $Fe_2O_4 Zn_{0.3} Ni_{0.7}$  بطريقة الترسيب الكيميائي عند درجات حرارة تليدين ( $1200^{\circ}C$  and  $1100^{\circ}C$ ,  $1000^{\circ}C$ ,  $900^{\circ}C$ ,  $800^{\circ}C$ ,  $700^{\circ}C$ ) على التوالي. اذ تبين تأثير درجات حرارة التليدين المختلفة على التحليل الطيفي والهيكل لمركبات  $Fe_2O_4 Zn_{0.3} Ni_{0.7}$ , اذ لوحظ من تقنية فحص حيود الاشعة السينية ان جميع النماذج ذات هيكل مكعبي اسبنلي والمسافات البينية للمستويات هي لها نفس معاملات ميلر (2.517, 2.958, 2.422, 2.093, 1.717, 1.613, 1.481 و 1.279) نانومتر. اما الممانعة الطيفية فهي اداة لفهم المساهمات المختلفة في الخصائص الكهربائية لأشباه الموصلات. اذ من خلال بيانات السماحية المعقدة والمعقدة - المعقدة ومعامل المعقد تم فهم المساهمات المتمثلة بالحبوب والحبوب الحبوب في الخصائص الكهربائية للنماذج. كما تم دراسة التحليل الطيفي للممانعة كدالة للتردد (1 كيلو هرتز - 5 ميجا هرتز) لمركب  $Fe_2O_4 Zn_{0.3} Ni_{0.7}$ . اذ اظهر الجزء الخيالي من الممانعة كدالة للتردد يظهر ديببي مثل الاسترخاء. وأظهرت رسومات Cole-Cole (تمثل العلاقة بين الجزء الحقيقي والجزء الخيالي للممانعة المعقدة) نوع غير (Debye) من الاسترخاء الزمني للعازل.

الكلمات الدالة: نيكل - زنك فرايت , حيود الاشعة السينية , قياسات ثابت العزل , الممانعة الطيفية.

## 1. Introduction

Ferrites materials are the fifth class of magnetic materials. The basis of these materials is the mixing of different metal oxides with ferric oxide and their main components known as ferrites. Ferrites are of great technical importance because they exhibit a spontaneous magnetic property under room temperature. The requirements of electronic and magnetic properties in advanced electronic and microwave devices have focused the attention of ferrite researchers [1-3]. Ferrites are the salts of transition metals, as their contents crystallize on known magnetic elements. The chemical formula of ferrites can be written as  $AB_2O_4$ , where A is a divalent metal ion-valence, B is  $Fe^{2+}$  and O is a bivalent oxygen ions. In the spinel structure, oxygen atoms are closely packed in the face-centered networks in the joints where the metal ions are distributed. This type of material possesses a momentary imbalance between the two spins produced by the magnetic interaction of atoms [4-5]. The technological applications of ferrite is its use in high frequency transformers and pulse, induction, coil deflection and applications in high permeability and low loss at high frequencies [6-7]. To study the effect of different temperature on structural analysis, the insulating and magnetic properties of Ni-Zn ferrites prepared a combustion reaction studied by K. Ramakrishna et al [8]. Application of complex spectroscopy analysis technique, results show Get it one half circular shape at each temperature over the measurement range, meaning that the electrical process responds to a single relaxation mechanism. The impedance and related coefficients of the electrical equivalent circuit depend on the temperature and microscopic structure of the samples. Constant isolation and loss of isolation of the probe samples are dominated by the conduction and relaxation processes associated with the grain boundary mechanism [10]. Complex resistance and dielectric properties of  $Mg_{0.5}Zn_{0.5}Fe_2O_4$  ferrite was measured in the frequency range (13-15 MHz) at several temperatures within the limits (0-100°C) and complex - complex resistance spectra indicating that the material could be represented by a For a two-layer leak capacitor that corresponds to bulk phenomena and granular boundaries at high and low frequencies respectively, and a string resistance of approximately the same value is observed at all temperatures. This resistance is believed to be due to external connections and electrodes. The capacitive element depends on the frequency and the insulation results are discussed The true  $\epsilon'_r$  insulation and loss of  $\epsilon''_r$  insulation at low frequencies is attributed to interstitial polarization, at high frequencies Debye as the relaxation of the directed polarization is dominant. It discusses the adoption of resistance and insulating

properties at temperature and frequency [10-11]. Spectral impedance is applied to investigate the attenuation of the sample electrical insulation at a temperature range of 323 to 473 K and at a frequency range of 42 Hz to 1.1 MHz. The complex impedance - impedance plot was analyzed by an equivalent circuit consisting of two connected R-cup units, each containing R (R) and constant phase (K). The Cole-Cole model is used to investigate the mechanism of buffer relaxation in the sample. Frequency-dependent conductivity spectrums obey the energy law [12]. Today the nano-ferrite scale has attracted a large number of researchers because of its unusual physical and chemical properties of it in bulk form. The current work of this paper deals with the composition and study of nanocrystalline  $\text{Ni}_{0.7}\text{Zn}_{0.3}\text{Fe}_2\text{O}_4$  samples heated in 700°C, 800°C, 900°C, 1000°C, 1100°C and 1200°C receptively synthesized co-perception method. X-ray analysis is performed to confirm phase formation, structure determination and particle size. The properties of the dielectric are studied to understand the conduction phenomenon. The impedance spectral analysis method is used to analyze the frequency response of the  $\text{Ni}_{0.7}\text{Zn}_{0.3}\text{Fe}_2\text{O}_4$  structures in the 100Hz-5MHz vibrational frequency range. It is proposed to conduct an equivalent circuit to calculate the observed results.

## 2. Experimental techniques

### 2.1 Sampling preparation

Salts of precursors, nickel nitrate [ $\text{Ni}(\text{NO}_3)_2 \cdot 6\text{H}_2\text{O}$ ], Zinc Acetate [ $\text{Zn}(\text{CH}_3\text{COO})_2 \cdot 4\text{H}_2\text{O}$ ] ferric nitrate [ $\text{Fe}(\text{NO}_3)_3 \cdot 9\text{H}_2\text{O}$ ] With each analytical purity, pour in a cup to melt them into distilled water. These salts are dissolved in distilled water by adding some amount of hydrochloric acid and obtained a clear solution to the salts. The cup containing this solution was then kept on a magnetic stirrer (making Remy) for continuous stirring and heating at 60°C for 2 hours for uniform mixing of raw materials to obtain a clearer and homogeneous solution again. After obtaining a homogeneous solution 1M sodium hydroxide solution was added drop by drop to the above solution. The amount of sodium hydroxide to be added over the homogeneous (clear) solution is determined. The deposit was obtained with the color change from brown to black as we go to form  $\text{Ni}_{0.7}\text{Zn}_{0.3}\text{Fe}_2\text{O}_4$  sample. The precipitation reaction was performed at 60°C and pH=12. The precipitate was washed and filtered with distilled water several times until the pH of the filter became 7. Thus the wet powders (residues) of  $\text{Ni}_{0.7}\text{Zn}_{0.3}\text{Fe}_2\text{O}_4$  sample by a common chemical technique in the precipitation. Initially, wet powders of the ferrite were kept in the furnace to pre-simmer at 100°C for 4

hours for 8 hours and cooled slowly to maintain uniform cooling. This stage of sintering is called before sintering. Pre-sintered samples of ferrite are then taken in a clean agate mortar and milled with a pestle for at least one hour. To prepare the pellet, add a drop (2-3 drops) of an organic reagent called polyvinyl alcohol (PVA) to a small amount of ferrite powder and then grind this mixture to mix a uniform PVA in powder. This powder is poured in diameter and a 10 mm diameter punch is pressed into the hydraulic press machine. Pressure of 5-6 ton / cm<sup>2</sup> was applied for 10 min. Powders were pressed and compressed into dense pellets. The pellets were then prepared for 700°C, 800°C, 900°C, 1000°C, 1100°C and 1200°C, and various profiles as Ni<sub>0.7</sub>Zn<sub>0.3</sub>Fe<sub>2</sub>O<sub>4</sub> characterization. We chose the Ni<sub>0.7</sub>Zn<sub>0.3</sub>Fe<sub>2</sub>O<sub>4</sub> sample for current work due to their need for growing electrical and electronic technology. We have studied the preparation of ferrite materials and optimized various processing steps that meet the practical demands and confirm the formation of its phase and magnetic properties is the main subject of the legitimate work. The following studies are conducted during this working session.

## 2.2 Structural Analysis by X-ray Diffraction Technique:

XRD patterns of Ni<sub>0.7</sub> Zn<sub>0.3</sub> Fe<sub>2</sub>O<sub>4</sub> samples were obtained using X-ray diffractometer technique (model Bruker D8 Advance) with CuK $\alpha$  radiation ( $\lambda=1.5418 \text{ \AA}$ ). The patterns were characterized by using for Ni-ferrite and Zn-ferrite. The average size of the crystals was determined from the width of the maximum diffraction limits using the Deby-Schichter formula [13].

$$D_p = \frac{k\lambda}{\beta \cos \theta} \quad (1)$$

where  $k = 0.89$  (assuming the particles are spherical in shape);  $\lambda$  = wavelength of X-ray diffraction;  $\beta$  = full width at half maximum ( FWHM ) OF the diffraction peak; and  $\theta$  = angle of diffraction.

Assuming that all the particles to be spherical, the specific surface area of particles was calculated by relationship [14].

$$S = \frac{6000}{d\rho} \quad (2)$$

Where S = the specific surface area of particles, d = the diameter of the crystallite in nm and  $\rho$  = the density of the particle in  $\text{g cm}^{-3}$ .

### 2.3 Dielectric measurements:

Using two methods of investigation, the insulating measurements of the samples, namely the dielectric constant, which in turn depends on the parallel capacitance resulting from the models and the loss of insulation using a tensile meter (model Hickey 3532-50 Lear Hetister) in the frequency band 1 kHz-1 MHz. For insulator measurements, samples were used in the form of a pellet with a thickness of  $t = 0.2$  cm and a diameter of 1 cm. The two faces of the pellet were coated with silver paint, which acts as a condenser consisting of two parallel plates. The condenser is even formed firmly fixed in the sample copper holder electrodes with the help of a bolt nut system.

### 2.4 Impedance spectroscopy analysis:

Electrolysis Using the S-spectrum spectrum technique, electrical behavior of the system was studied over a wide range of frequencies. This method enables us to separate the real components and imaginary electrical transactions, thus providing a true picture of the material properties. Using the impedance spectrum method, the properties of grains and granules in polycrystalline material can usually be considered as two consecutive circuits in the representation of data. The data can be analyzed in terms of four possible complex formalities, complex impedance,  $Z^*$ , complex complex,  $M^*$ , constant electrical insulation, and dielectric loss used in current studies. They are related to each other as follows [15-16].

$$Z^*(\omega) = Z' - j Z'' = R_s - j / \omega C_s \quad (3)$$

$$M^*(\omega) = M' - j M'' = j \omega C_o Z^* \quad (4)$$

$$\tan\delta = \epsilon^*(\omega) = M' - j M'' = j \omega C_o Z^* \quad (5)$$

in the present study we have used following relations to calculate Modulus and impedance

$$M' = \epsilon' / (\epsilon'^2 + \epsilon''^2) \quad (6)$$

$$M'' = \epsilon'' / (\epsilon'^2 + \epsilon''^2) \quad (7)$$

$$Z' = M'' / \omega C_o \quad (8)$$

$$Z'' = M' / \omega C_0 \quad (9)$$

Where

$Z'$ ,  $Z''$  = The real and imaginary parts of the complex impedance.

$M'$ ,  $M''$  = The real and imaginary parts of the complex impedance.

$\epsilon'$ ,  $\epsilon''$  = The real and imaginary parts of the dielectric constant.

$\tan \delta$  = The dielectric loss.

$\epsilon^*$  = The dielectric complex.

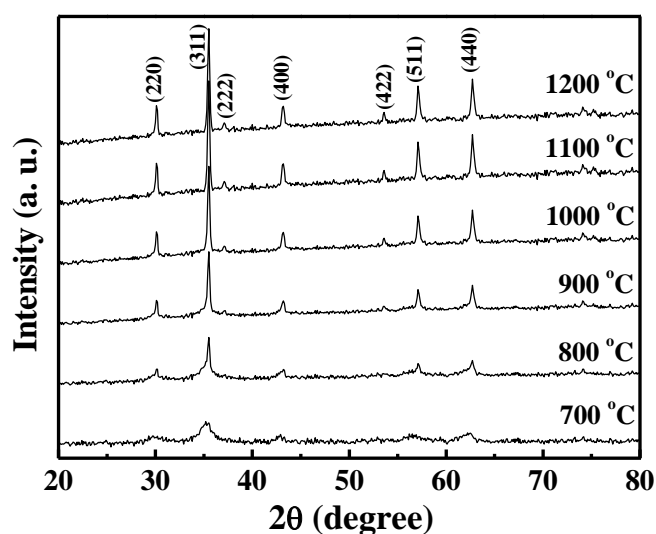
$\omega$  = The angular velocity ( $\omega = 2\pi f$ ).

An electrical response of the samples can be analyzed via complex dielectric modulus formalism  $M^*(\omega)$ , which is an attractive approach based on polarization analysis.

### 3. Results and discussion

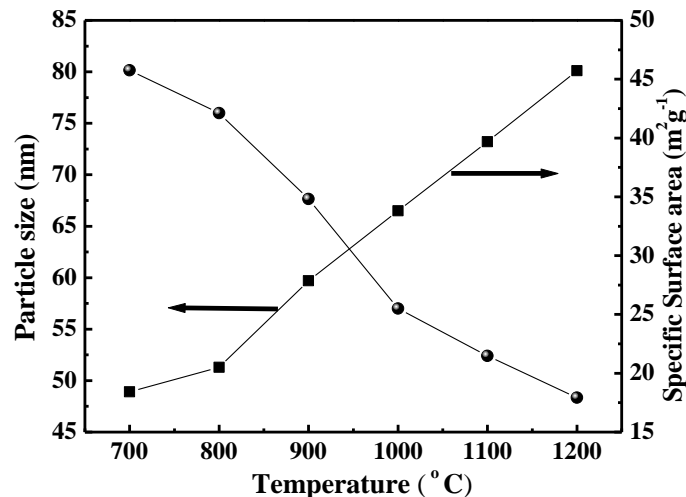
#### 3.1 Structural analysis by XRD

**Fig. (1).** x-ray diffraction patterns of  $\text{Ni}_{0.7}\text{Zn}_{0.3}\text{Fe}_2\text{O}_4$  ferrites in 700°C, 800°C, 900°C, 1000°C, 1100°C and 1200°C respectively. It was reveals that nanoparticles are of a single phase. No peak of impurity was observed in x-ray diffraction pattern ensure sample purity. The card No. ( 10-325) for Ni-ferrite and Card No. (22-1086) for Zn-ferrite was used to index all peaks in Ni-Zn pattern [19].



**Fig. (1):** x-ray diffraction patterns of  $\text{Ni}_{0.7}\text{Zn}_{0.3}\text{Fe}_2\text{O}_4$  ferrites in different temperature.

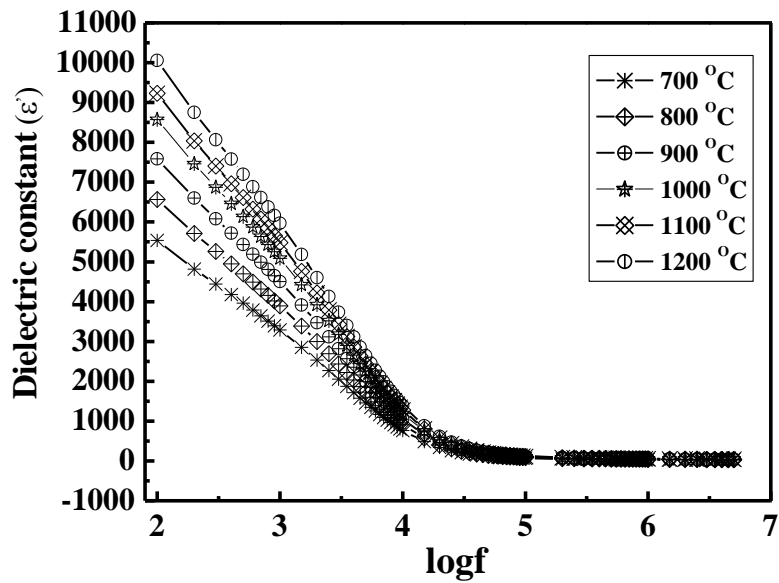
The value of the lattice parameter was found to be ( 8.366 ~ 8.376 Å). This value corresponds to the previous values reported [18]. The particle size was calculated to be ( 49 – 81) nm of full width half the maximum of the strongest peak (311) of the XRD pattern employing the Shearer's formula [19]. Similar explanation in case  $\text{Ni}_{0.4}\text{Zn}_{0.2}\text{Mn}_{0.4}\text{Fe}_2\text{O}_4$  by K.Praveena, et. al. [20].



**Fig. (2):** Particle size difference and specific area with treatment temperature of  $\text{Ni}_{0.7}\text{Zn}_{0.3}\text{Fe}_2\text{O}_4$  ferrites.

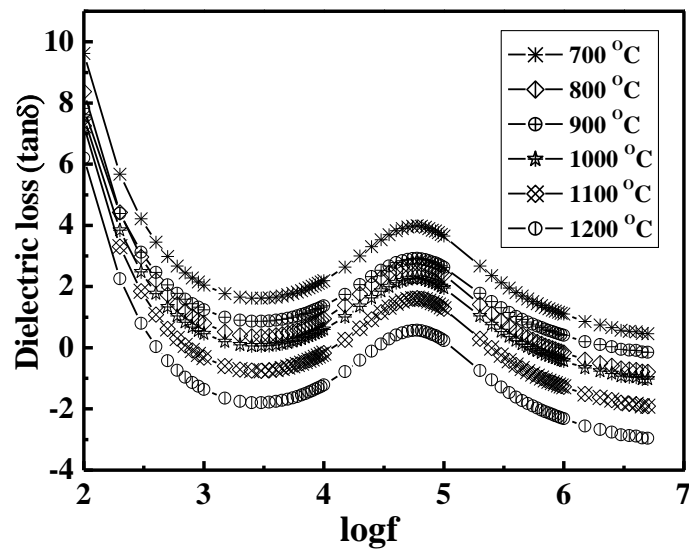
### 3.2 Dielectric properties:

Fig. (3) shows the constant variation of electrical insulation ( $\epsilon'$ ) with frequency at different temperatures. From the plot it can be observed that the dielectric constant decreases rapidly with increased frequency but after 1 cathode remains fairly constant for all samples. The isolating behavior of the current samples can be explained on the basis that the mechanism of polarization in ferrite is similar to the conduction process. The electron exchange  $\text{Fe}^{3+} \leftrightarrow \text{Fe}^{2+}$  gives the local transmission of electrons in the direction of the applied electric field, leading to polarization in the ferrite. In the natural insulator behavior, the dielectric constant decreases with the frequency increase up to a constant value, depending on the fact that after a certain frequency of the electrode field the electron exchange does not follow the alternating field [21].



**Fig. (3):** Frequency dependent variation of dielectric constant for  $Ni_{0.7}Zn_{0.3}Fe_2O_4$  ferrites at different temperature.

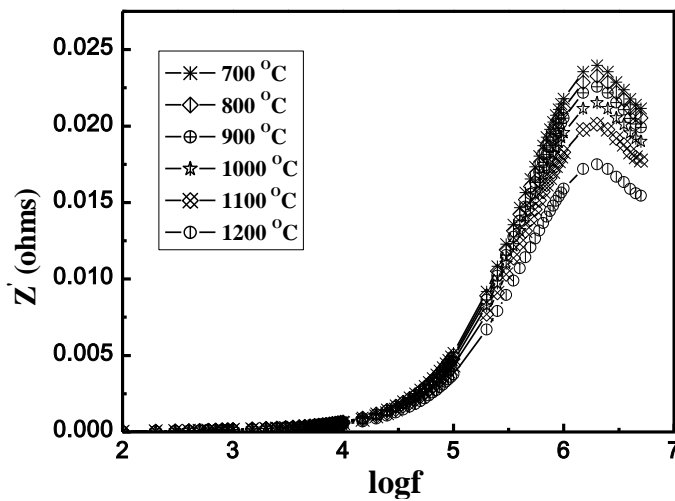
The difference of shadow loss ( $\tan\delta$ ) with frequency at room temperature is shown in Fig. (4). Contrast is similar to change Increase in frequency and temperature.



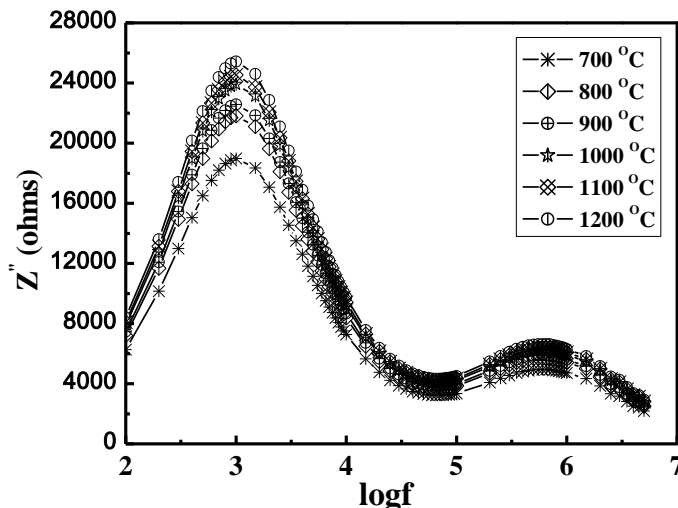
**Fig.(4):** Frequency dependent variation of dielectric loss for  $Ni_{0.7}Zn_{0.3}Fe_2O_4$  ferrites at different temperature.

This also indicates a single relaxation process in Fig. (5) showing the variation in the real portion of the resistance ( $Z'$ ) with frequency at different temperatures. As can be seen, the

width of the curves in  $Z'$  value is reduced with frequency at all temperatures. The amount of  $Z'$  decreases with the temperature indicating an increase in the AC conductivity of the alternating current. Fig. (5) shows the difference in the imaginary part of  $Z$  resistance with frequency at different temperatures. Peak in  $Z''$  turns to low frequencies with increased temperature indicating a lower relaxation in the system. Relaxation times are calculated from the frequency at which Maxima is observed. The maximum limit is found to increase with the temperature indicating a loss increase in the sample [22-23].

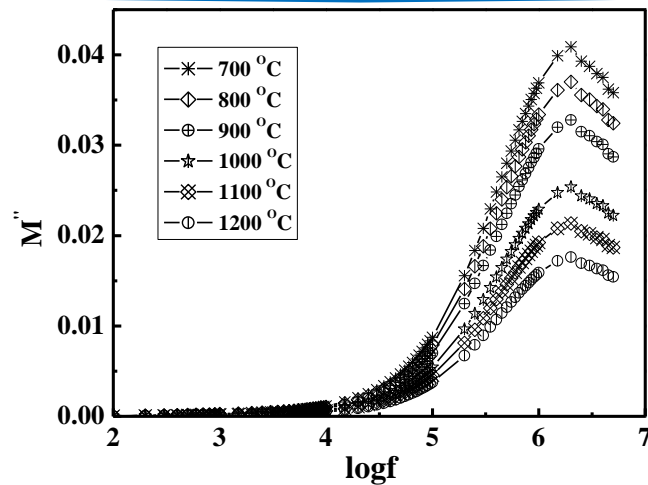


**Fig. (5):** Frequency dependent variation of ( $Z'$ ) at different temperature for  $Ni_{0.7}Zn_{0.3}Fe_2O_4$  ferrites.

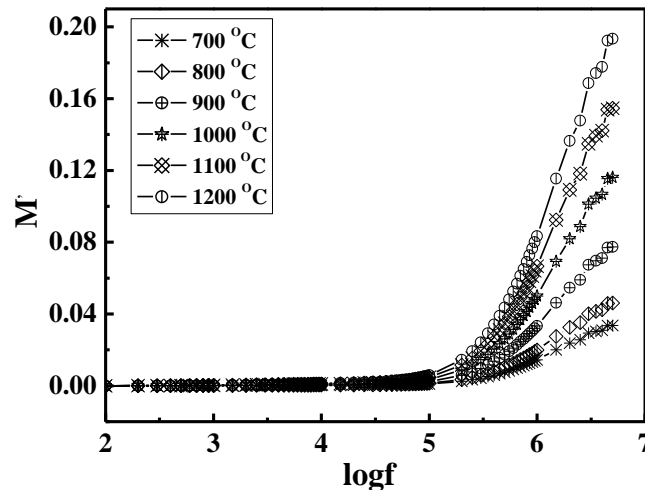


**Fig. (6):** Frequency dependent variation of imaginary ( $Z''$ ) parts of the complex impedance at different temperature for  $Ni_{0.7}Zn_{0.3}Fe_2O_4$  ferrites.

Fig. (7) shows the frequency dependence of  $M''$  in a different amplifier. It is noted that the value of  $M''$  is very low in the low frequency zone. Continuous increase in  $M''$  dispersion with increased frequency shows the tendency to saturation in the maximum value of the oscillator per sintering sintering. The saturation trend supports the suggestion that short-range carrier traffic is a delivery process. These explanations may be related to the absence of a recovery force leading to the movement of the charge carriers within the induced electric field. Low-value  $M''$  in the low-frequency side supports conduction phenomena due to the long-range mobility of the carrier's shipments, as well as that electrolysis makes a small contribution in the material [24]. In the conduction process, the holes contribute smaller than those electrons because of their low mobility. The electron between the iron  $Fe^{2+}$  and  $Fe^{3+}$  ions, leading to the local transition in the direction of the extruded electrode field (while the exchange of the hole between  $Ni^{3+}$  and  $Ni^{2+}$ , causes electrostatic polarization in the ferrite [25]. However, exchanges between  $Ni^{2+}$  and  $Fe^{3+}$  can also be found. However,  $Fe^{2+} \Leftrightarrow Fe^{3+}$  is the easiest and therefore their number will be reflected in a fixed dielectric value, and the results of Fig. (7) indicate that this figure should be the same for all measurements The forms of the spectral pieces obtained at different temperatures are still the same Thus, the distribution of relaxation time is independent of the temperature Fig. (8) shows the dependence on  $M'$  frequencies at different temperature values. It is observed from the figure that the increase with  $M'$  increases with frequency increase except for the emergence of a small and wide band that turns out to be high frequency side-by-side with an increase in the temperature. cm area of the frequency below the peak. The maximum limit determines the range of charge carriers due to long-range jump. At frequencies above the maximum peak (upper frequency), the carriers are limited to potential wells and are traveling at a short distance [24]. Similar explanation in case  $CuFe_2O_4$  by Sakia Shaikh et. al. [25].



**Fig. (7):** Frequency dependent variation of imaginary ( $M''$ ) parts of the complex modulus at different temperature for  $Ni_{0.7}Zn_{0.3}Fe_2O_4$  ferrites.



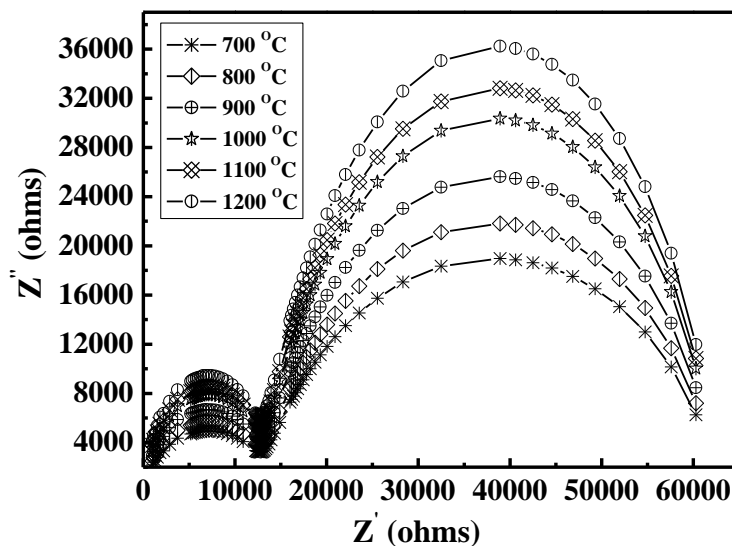
**Fig. (8):** Frequency dependent variation of real ( $M'$ ) parts of the complex impedance at different temperature for  $Ni_{0.7}Zn_{0.3}Fe_2O_4$  ferrites.

Fig. (9) shows the composite impedance level plots measured at 700 °C, 800°C, 900 °C, 1000°C, 1100°C and 1200°C, respectively. Each curve consists of two semicircles, one small and one large. One small at low frequencies indicates the effect of large grain boundaries and one at high frequencies reflecting the grain effect. Each half circle is represented by a parallel exponential circle that corresponds to the individual components of the material [8, 26]

#### 4. Conclusions

Samples  $Ni_{0.7}Zn_{0.3}Fe_2O_4$  showing the structure of the spinel and cube (311) peak is more intense. The intensity of peak samples varies with different temperature particle size, the

specified surface area was calculated through normal procedures 4. The difference of static insulation and insulation loss with frequency shows dielectric dissipation in  $\text{Ni}_{0.7}\text{Zn}_{0.3}\text{Fe}_2\text{O}_4$ . Analysis of electrical and inertial data by complex impedance ( $Z^*$ ) and buffer coefficient ( $M^*$ ) provides more ideas in the behavior of materials, information on grain and grain contribution input resistance and amplitude of electricity properties of samples.



**Fig. (9):**  $Z''$  vs  $Z'$  plots for  $\text{Ni}_{0.7}\text{Zn}_{0.3}\text{Fe}_2\text{O}_4$  ferrites at different temperature.

## References

- [1] S. O. Pillai, "Solid State Physics", six<sup>th</sup> edition, New Revised (2010).
- [2] S. Prasad, N. S. Gajbhiye, "(HF, Zr)<sub>2</sub>Fe and Zr<sub>4</sub>Fe<sub>2</sub>O<sub>6</sub> compounds and their hydrides: phase equilibria, crystal structure and magnetic properties", J. Alloys Compd 265, 87, (1998).
- [3] J. B. Dasilva and N. D. S. Mohallem, "Preparation of Composites of Nickel Ferrites Dispersed in Silica Matrix", Journal of Magnetism and Magnetic Materials, 226, 1393, (2001).
- [4] P. Moriarty, "Nanostructured Materials", Rep. Prog. Phys. 64, 297, (2001).
- [5] [C. Y. Tsay, K. S. Liu, T. F. Lin and I. N. Lin, "Microwave Sintering of NiCuZn Ferrites and Multilayer Chip Inductors", Journal of Magnetism Materials, 209, 189, (2000).
- [6] P. Vijaya Bhasker Reddy, B. Ramesh, Ch. Gopal Reddy, "Electrical conductivity and dielectric properties of Zinc substituted lithium ferrites prepared by sol-gel method" Physica B: Cond. Matter, 405, 1852, (2010).

- [7] F. Kubel, H. Schmid, "*Structure of ferroelectric and ferroelastic monodomain crystal of perovskite BiFeO<sub>3</sub>*" ,Acta crystallographica B: 46, 698, (1990).
- [8] K. Ramakrishna, K. Vijaya Kumar, C. Ravindernathgupta, Dachehalli Ravinder," *Magnetic properties of Ni-Zn ferrites by citrate Gel method*", *Advances Materials Physics and chemistry*, 2, 149, (2012).
- [9] R. Das, T. Sarkar and K. Mardal, "*The velocity-dependent attenuation, measured as a function of bulk flow velocity at 1.5, 1.8, and 2.0 K, is compared with data from other researchers*" J. Phys. D: Appl. Phys, 45, 455 (2012).
- [10] M. H. Abdullah, A. N. Yusoff, "*Domain size correlated magnetic properties and electrical impedance of size dependent nickel ferrite nanoparticles*",*Journal of Alloys and Compounds*, 2332, 129 (1996).
- [11] R. A. Mondal, B.S. Murty and V.R.K. Murthy, "*Complex impedance and dielectric properties of an Mg Zn ferrite*" "*current Applied Physics*", 4, 1727 (2014).
- [12] B. L. Patil, S. R. Sawant, S. A. Patil and R. N. Patil, "*Maxwell–Wagner polarization in grain boundary segregated NiCuZn ferrite*", J. Phys., 43, 179 ( 1993 ).
- [13] K. M. Batoor, M. S. Ansari, "*The x-ray diffraction analysis of the samples was carried out using Fe-K $\alpha$  radiation*", *Nano scale Res. Lett*, 7, 1 (2012).
- [14] D. Meyer hofere, "*The Production of High Speed Light Ions Without the Use of High Voltages*", *Physical review*, 112, 58 (2011).
- [15] Baljinder Kaur, Lakhbir Singh, V. Annapu Reddy, Dae-Young Jeong, Navneet Dabra, Jasbir S. Hundal, "*AC Impedance Spectroscopy, Conductivity and Optical Studies of Sr doped Bismuth Ferrite Nanocomposites*" "*Int. J. Electrochem. Sci*", 11, 4120 (2016).
- [16] F. Gheorghiu, M. Calugaru, A. Iancu Iescu, V. Musteata, L. Mitoseriu, "*Preparation and functional characterization of BiFeO<sub>3</sub> ceramics: A comparative study of the dielectric properties*", *Solid State Sciences*, 123, 79 (2013).
- [17] K. Rafeekali, Mohammed Maheem, E.M. Mohammed, "*Effect of Sintering Temperature on the Structural and Magnetic Properties of Nickel Ferrite Nanoparticles*" *International Journal of Engineering Science and Innovative Technology (IJESIT)*, 4, 34 (2015).
- [18] R. K. Panda, R. Muduli, S. K. Kar, D. Behera, "*Dielectric relaxation and conduction mechanism of cobalt ferrite nanoparticles*", *Journal of Alloys and Compounds*, 615, 899 (2014).

- [19] C. Hammond, "*The Basic of Crystallography and Diffraction*", Oxford University Press, Oxford, (2001).
- [20] Navneet Singh, Ashish Agarwal, Sujata Sanghi, Satish Khasa, "*conductivity relaxation process and magnetic properties of Mg substituted Ni–Cu ferrites*", Journal of Magnetism and Magnetic Materials 324, 2506 (2012).
- [21] Khalid Mujasam Batoo, Feroz Ahmed, Mir, M. S. Abd El-Sadek, M. D. Shahabuddin, Niyaz Ahmed, "*Domain size correlated magnetic properties and electrical impedance of size dependent nickel ferrite nanoparticles*", AIP Advances, 5, 017119, (2015).
- [22] D. Arcos, M. Vazquez, M. Valenzuela, "*Effects of grain size distribution on Cole-Cole plots of polycrystalline spinels*", J. Mater. Res, 3, 861 (1999).
- [23] M. R. Biswal, J. Nanda, N. C. Mishra, S. Anwar, A. Mishra, "*Influence of Fe substitution on structural and electrical properties of Gd orthochromite ceramics*", Adv. Mat. Lett, 5(9), 537 (2014).
- [24] F. Gheorghiu, M. Calugaru, A. Iancu Iescu, V. Musteata, L. Mitoseriu, "*Conductivity and Optical Studies of Sr doped Bismuth Ferrite Nanocomposites*", Solid State Sciences, 123, 79 (2013).
- [25] Sakia Shabnam Kader, Deba, Prasad Paul and Shaikh Manjum Hoque, "*Effect of Temperature on the Structural and Magnetic Properties of CuFe<sub>2</sub>O<sub>4</sub> Nano Particle Prepared by Chemical Co-Precipitation Method*" ,International Journal of Materials, Mechanics and Manufacturing, 2, 173 (2014).
- [26] M. R. Biswal, J. Nanda, N. C. Mishra, S. Anwar, A. Mishra, "*Dielectric and impedance Spectroscopic studies of multiferroic BiFe<sub>1-x</sub>Ni<sub>x</sub>O<sub>3</sub>*" Adv. Mat. Lett. 5, 531 (2014).